Journal of Organometallic Chemistry 694 (2009) 2142–2152

Contents lists available at ScienceDirect

Journal of Organometallic Chemistry

journal homepage: www.elsevier.com/locate/jorganchem

Crystal and solution structures of di-*n*-butyltin(IV) complexes of 5-[(*E*)-2-(4-methoxyphenyl)-1-diazenyl]quinolin-8-ol and benzoic acid derivatives: En route to elegant self-assembly via modulation of the tin coordination geometry

Tushar S. Basu Baul [a,*], Archana Mizar [a], Anup Paul [a], Giuseppe Ruisi [b], Rudolph Willem [c], Monique Biesemans [c], Anthony Linden [d,*]

[a] Department of Chemistry, North-Eastern Hill University, NEHU Permanent Campus, Umshing, Shillong 793 022, India
[b] Dipartimento di Chimica Inorganica e Analitica "Stanislao Cannizzaro", Università di Palermo, Viale delle Scienze, Parco D'Orleans II, Edificio 17, 90128 Palermo, Italy
[c] High Resolution NMR Centre (HNMR), Department of Materials and Chemistry (MACH), Vrije Universiteit Brussel (VUB), Pleinlaan 2, B-1050 Brussel, Belgium
[d] Institute of Organic Chemistry, University of Zurich, Winterthurerstrasse 190, CH-8057 Zurich, Switzerland

ARTICLE INFO

Article history:
Received 22 January 2009
Received in revised form 13 February 2009
Accepted 16 February 2009
Available online 4 March 2009

Keywords:
5-[(*E*)-2-(4-methoxyphenyl)-1-diazenyl]quinolin-8-ol
Di-*n*-butyltin(IV) complexes
Benzoic acid
Mixed ligands
Solution and solid-state tin NMR
Crystal structure

ABSTRACT

Reactions of $^{n}Bu_2SnCl(L^1)$ (**1**), where L^1 = acid residue of 5-[(*E*)-2-(4-methoxyphenyl)-1-diazenyl]quinolin-8-ol, with various substituted benzoic acids in refluxing toluene, in the presence of triethylamine, yielded dimeric mixed ligand di-*n*-butyltin(IV) complexes of composition $[^{n}Bu_2Sn(L^1)(L^{2-6})]_2$ where L^2 = benzene carboxylate (**2**), L^3 = 2-[(*E*)-2-(2-hydroxy-5-methylphenyl)-1-diazenyl]benzoate (**3**), L^4 = 5-[(*E*)-2-(4-methylphenyl)-1-diazenyl]-2-hydroxybenzoate (**4**), L^5 = 2-{(*E*)-4-hydroxy-3-[(*E*)-4-chlorophenyliminomethyl]-phenyldiazenyl}benzoate (**5**) and L^6 = 2-[(*E*)-(3-formyl-4-hydroxyphenyl)-diazenyl]benzoate (**6**). All complexes (**1**–**6**) have been characterized by elemental analyses, IR, ^{1}H, ^{13}C and ^{117}Sn NMR and ^{119}Sn Mössbauer spectroscopy and their structures were determined by X-ray crystallography, complemented by ^{117}Sn CP-MAS NMR spectroscopy studies in the solid state. The crystal structure of **1** reveals a distorted trigonal bipyramidal coordination geometry around the Sn-atom where the Cl- and N-atoms of ligand L^1 occupy the axial positions. In complexes **2–5**, the molecules are centrosymmetric dimers in which the Sn-atoms are connected by asymmetric μ-O bridges through the quinoline O-atom to give an Sn_2O_2 core. The differences in the Sn–O bond lengths within the bridge range from 0.28 to 0.48 Å, with the longer of the Sn–O distances being in the range 2.56–2.68 Å and the most symmetrical bridge being in **5**. The carboxylate group is almost symmetrically bidentate coordinated to the tin atom in **5** (Sn–O distances of 2.327(2) and 2.441(2) Å), unlike the other complexes in which the distance of the carboxylate carbonyl O-atom from the tin atom is in the range 2.92–3.03 Å. The structure of **5** displays a more regular pentagonal bipyramidal coordination geometry about each tin atom than in **2–4**. In contrast, the centrosymmetric dimeric structure of **6** involves asymmetric carboxylate bridges, resulting in a different $Sn_2C_2O_4$ motif. The Sn–O bond lengths in the bridge differ by about 0.6 Å, with the longer distance involving the carboxylate carbonyl O-atom (2.683(2) and 2.798(2) Å for two molecules in the asymmetric unit). The carboxylate carbonyl O-atom has a second, even longer intramolecular contact to the Sn-atom to which the carboxylate group is primarily coordinated, with these Sn···O distances being as high as 3.085(2) and 2.898(2) Å. If the secondary interactions are considered, all the di-*n*-butyltin(IV) complexes (**2–6**) display a distorted pentagonal bipyramidal arrangement about each tin atom in which the *n*-butyl groups occupy the axial positions.

1. Introduction

The chemistry of organotin(IV) quinolin-8-olates has been known for a long time, even though the coordination number of the tin atom and the type of distortion of the coordination polyhedron in the solid state are still open issues. Consequently, the structures of only a few organotin(IV) quinolin-8-olate(s) have been investigated so far, and among these, the diorganotin(IV) *bis*(quinolin-8-olate) group of compounds has received most of the attention. The crystal structures of R_2SnL_2 complexes, where R = Me [1], *p*-ClPh and *p*-MePh [2], ^{n}Bu and Cl [3], ^{n}Bu [4,5], ^{t}Bu [4], Ph [6,7] and Bz [8] revealed molecules with a highly distorted octahedral coordination of the tin atom by bidentate quinolin-8-olate

* Corresponding authors. Tel.: +91 364 2722626; fax: +91 364 2721000 (T.S. Basu Baul); tel.: +41 44 635 4228; fax: +41 44 635 6812 (A. Linden).
E-mail addresses: basubaul@nehu.ac.in, basubaul@hotmail.com (T.S. Basu Baul), alinden@oci.uzh.ch (A. Linden).

0022-328X/$ - see front matter © 2009 Elsevier B.V. All rights reserved.
doi:10.1016/j.jorganchem.2009.02.021

groups and essentially *cis*-R groups. Structural information on $R_2SnX(L)$ type complexes (e.g. R = $EtCO_2Me$; X = Cl) [9] is also available. In addition, the di-*n*-butyltin(IV) complexes of the type $^nBu_2Sn(L)_2$ and $^nBu_2SnCl(L)$ (L = 5-[(*E*)-2-(aryl)-1-diazenyl)quinolin-8-ol) were tested *in vitro* across a panel of human cell lines *viz*., WIDR (colon cancer), M19 MEL (melanoma), A498 (renal cancer), IGROV (ovarian cancer) and H226 (non-small cell lung cancer), MCF7 (breast cancer), EVSA-T (breast cancer) [5]. The results clearly show that di-*n*-butyltin(IV) complexes are overall, but not for every cell line, more active than *cis*-platin and some of the complexes display a higher activity than several of the standard cytotoxic agents.

On the other hand, the chemistry and structural properties of organotin(IV) carboxylates have been studied extensively; however, their potential for the construction of new mixed ligand complexes has not been explored so widely, with known examples involving the $^-O_2CC_6H_4(N{=}C(H)C_6H_4NMe_2\text{-}4)\text{-}2$, $^-O_2CC_6H_4NH_2\text{-}2$ and $^-O_2CC_6H_4N^+H_3\text{-}2$ [10] 2,6-$(^-O_2C)_2C_5H_3N$ and $^-O_2C\text{-}CO_2^-$ [11], $^-O_2CC_6H_4(OH\text{-}2)(N{=}NC_6H_4(Cl\text{-}4)\text{-}5)$, $^-O_2CC_6H_4(OH\text{-}2)(N{=}NC_6H_4\text{-}(Me\text{-}4)\text{-}5)$ and $^-O_2CC_6H_4(OH\text{-}2)(N{=}NC_6H_4(Br\text{-}4)\text{-}5)$ [12], and 2-$ClC_6H_4CO_2^-$ and $^-O_2CC_5H_4N\text{-}2$ [13] ligands. They display distorted trigonal bipyramidal, skew-trapezoidal bipyramidal and pentagonal bipyramidal coordination geometries around the tin atom. In order to fill this void, given the synthetic and structural importance and the potential biological activity of organotin(IV) complexes in general [7,8,14], and di-*n*-butyltin(IV) complexes with 5-[(*E*)-2-(aryl)-1-diazenyl)quinolin-8-olates in particular [5], we initiated the exploration of the reaction products of $^nBu_2SnCl(L^1)$ (**1**) with various substituted benzoic acids. Besides the conventional spectroscopic analysis (IR, NMR (^1H, ^{13}C, ^{119}Sn) and ^{119}Sn Mössbauer) of the resulting mixed ligand complexes (**2**–**6**), this report evaluates the impact of the electronic and steric influence of the carboxylate residue attached to the tin atom on the structural characteristics of these complexes, as determined by X-ray crystallography and further complemented by ^{117}Sn CP-MAS NMR spectroscopy in the solid state and, for one of the complexes, by variable temperature NMR in solution. In addition, we also present the crystal structure of one of the reactants $^nBu_2SnCl(L^1)$ (**1**), which has not been reported so far [5]. Our results reveal a strong modulation of the tin coordination geometry as a function of the substituent pattern on the L^{2-6} ligand.

2. Experimental

2.1. Materials

$^nBu_2SnCl_2$ (Aldrich) was used as received. All the solvents used in the reactions were of AR grade and dried using standard procedures. Toluene was distilled from sodium benzophenone ketyl.

2.2. Physical measurements

Carbon, hydrogen and nitrogen analyses were performed with a Perkin Elmer 2400 series II instrument. IR spectra in the range 4000–400 cm^{-1} were obtained on a Perkin–Elmer Spectrum BX series FT-IR spectrophotometer with samples investigated as KBr discs. ^1H, ^{13}C and ^{117}Sn NMR spectra of the organotin(IV) compounds were recorded on a Bruker Avance 250 spectrometer and measured at 250.53, 63.00 and 89.27 MHz, respectively. The ^1H, ^{13}C and ^{117}Sn chemical shifts were referenced to Me_4Si set at 0.00 ppm, $CDCl_3$ set at 77.0 ppm and Me_4Sn set at 0.00 ppm, respectively. ^1H and ^{13}C NMR assignments have been achieved using standard 1D ^1H and ^{13}C NMR and gradient-assisted 2D ^1H–^{13}C heteronuclear multiple-quantum correlation (HMQC) and heteronuclear multiple-bond correlation (HMBC) spectroscopy, on the basis of the labelling scheme shown in Scheme 1. CP-MAS ^{117}Sn NMR spectra were recorded on the same instrument, equipped with a 4 mm MAS broad-band probe. ^{117}Sn was chosen instead of the more common ^{119}Sn nucleus, because of RF intereferences from a local radio station. Spinning frequencies are chosen between 7 and 9 kHz. A contact time of 1 ms and a recycling delay of 2 s were used. The chemical shift reference was set using $(cyclo\text{-}C_6H_{11})_4Sn$ (−97.35 ppm relative to $(CH_3)_4Sn$). The principal values of the ^{117}Sn chemical shielding tensors were determined by fitting the anisotropy pattern of the spinning side bands according to the Herzfeld–Berger formalism, using the 'dmfit' program (Massiot D. *dmfit program*; available at http://crmht-europe.cnrs-orleans.fr). The Mössbauer spectra were recorded with a conventional spectrometer operating in the transmission mode. The source was $Ca^{119}SnO_3$ (Ritverc GmbH, St. Petersburg, Russia; 10 mCi), moving at room temperature with constant acceleration in a triangular waveform. The driving system was obtained from Halder (Seehausen, Germany), and the NaI (Tl) detector from Harshaw (De Meern, The Netherlands). The multi-channel analyzer and the related electronics were purchased from Takes (Bergamo, Italy). The solid absorber samples, containing *ca.* 0.5 mg cm^{-2} of ^{119}Sn, were held at 77.3 K in a MNC 200 liquid-nitrogen cryostat (AERE, Harwell, UK). The velocity was calibrated using a ^{57}Co Mössbauer source (Ritverc GmbH, St. Petersburg, Russia, 10 mCi), and an iron foil as absorber. The isomer shifts are relative to room temperature $Ca^{119}SnO_3$. C–Sn–C angles determined from the Mössbauer spectra were calculated with p.q.s. [alkyl] = −1.03 mm s^{-1} [15].

2.3. Synthesis of ligands

The 5-[(*E*)-2-(4-methoxyphenyl)-1-diazenyl]quinolin-8-ol (L^1H), 2-[(*E*)-2-(2-hydroxy-5-methylphenyl)-1-diazenyl]benzoic acid (L^3H'), 5-[(*E*)-2-(4-methylphenyl)-1-diazenyl]-2-hydroxybenzoic acid (L^4H'), 2-{(*E*)-4-hydroxy-3-[(*E*)-4-chlorophenyliminomethyl]phenyldiazenyl}benzoic acid (L^5H') and 2-[(*E*)-2-(3-formyl-4-hydroxyphenyl)-1-diazenyl]benzoic acid (L^6H') were prepared and characterized by methods described in earlier reports [8,16–19] while benzoic acid (L^2H') was obtained from Aldrich. Note: H and H′ refer to the replaceable protons in the ligands L^1 and L^{2-6}, respectively.

2.4. Synthesis of the di-n-butyltin(IV) complexes

2.4.1. Synthesis of $^nBu_2SnCl(L^1)$ (**1**)

Complex **1** was prepared by reacting equimolar amounts of L^1Na (generated *in situ* using sodium methoxide in anhydrous methanol) and $^nBu_2SnCl_2$ in anhydrous benzene, as described elsewhere [5]. The product was recrystallized from benzene–hexane (v/v 1:1), affording pure orange crystals (M.p.: 72–74 °C) of **1**. This sample was used for the subsequent syntheses.

2.4.2. Synthesis of $[^nBu_2Sn(L^1)(L^{2-6})]_2$

A typical procedure for the synthesis of mixed ligand complexes of the type $[^nBu_2Sn(L^1)(L^{2-6})]_2$ is described below.

*2.4.2.1. Synthesis of $[^nBu_2Sn(L^1)(L^2)]_2 \cdot 0.33(C_6H_{12})$ (**2**).* L^2H' (0.13 g, 1.06 mmol) in hot anhydrous toluene (40 mL) was added to a hot anhydrous toluene solution (30 mL) of $^nBu_2SnCl(L^1)$ (**1**) (0.50 g, 1.08 mmol). The reaction mixture was refluxed for one hour; triethylamine (0.11 g, 1.08 mmol) was then added drop-wise and reflux was continued for additional 3 h. The reaction mixture was cooled to room temperature and filtered in order to remove $Et_3N \cdot HCl$. The filtrate was evaporated and the residue dried *in vacuo*. The residue was extracted into a benzene and hexane mixture (v/v 1:1) and filtered to remove any suspended particles. The filtrate was concentrated and allowed to evaporate slowly at room temperature until the solid material precipitated. The solid was fil-

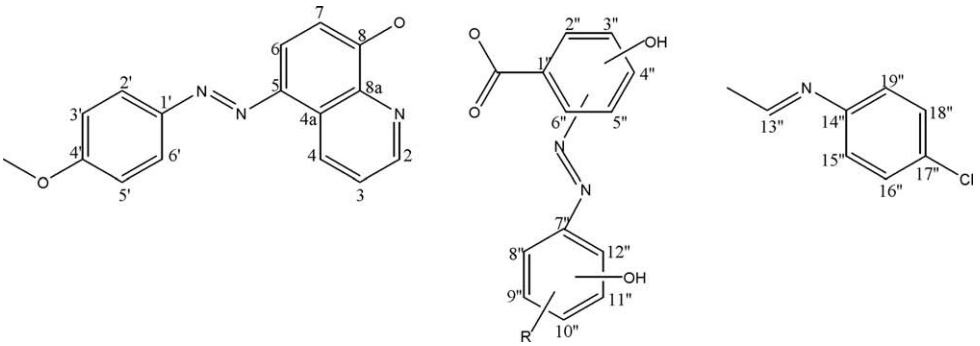

Scheme 1. Structures of the ligands and the numbering protocol.

tered, dried *in vacuo* and then recrystallized from a mixture of chloroform–cyclohexane (v/v 1:1), which upon slow evaporation afforded pure red crystals. Yield: 0.38 g (55.8%), M.p. 102–103 °C. Anal. Calc. for $C_{64}H_{74}N_6O_8Sn_2$: C, 59.46; H, 5.77; N, 6.50. Found: C, 60.01; H, 5.80; N, 6.31%. IR (KBr, cm^{-1}): 1245 ν(C(aryl)O, 1603 $\nu(OCO)_{asym}$. ^{119}Sn Mössbauer data: δ = 1.46, Δ = 3.79, $\Gamma\pm$ = 0.83 mm s^{-1}, calculated C–Sn–C = 153° (X-ray: 152.0(1)).

The other mixed ligand complexes (^{n}Bu$_2$Sn(L^1)(L$^{3-6}$) (**3**–**6**) were prepared by reacting **1** with the appropriate conjugated acids of the ligands (L^{3}H′–L^{6}H′) using analogous procedures.

*2.4.2.2. Synthesis of [^{n}Bu$_2$Sn(L^1)(L^3)]$_2$ (**3**).* Red plates of **3** were obtained from benzene–hexane (v/v 1:1). Yield: 0.56 g (68.3%), M.p. 103–104 °C. Anal. Calc. for $C_{76}H_{82}N_{10}O_{10}Sn_2$: C, 59.55; H, 5.39; N, 9.14. Found: C, 60.12; H, 5.50; N, 8.96%. IR (KBr, cm^{-1}): 1249 ν(C(aryl)O, 1598 $\nu(OCO)_{asym}$. ^{119}Sn Mössbauer data: δ = 1.44, Δ = 3.79, $\Gamma\pm$ = 0.76 mm s^{-1}, calculated C–Sn–C = 153° (X-ray: 153.6(1)).

*2.4.2.3. Synthesis of [^{n}Bu$_2$Sn(L^1)(L^4)]$_2$ (**4**).* Orange crystals of **4** were obtained from toluene–chloroform (v/v 1:1). Yield: 0.43 g (52.4%), M.p. 155–157 °C. Anal. Calc. for $C_{76}H_{82}N_{10}O_{10}Sn_2$: C, 59.55; H, 5.39; N, 9.14. Found: C, 60.01; H, 5.57; N, 8.96%. IR (KBr, cm^{-1}): 1255 ν(C(aryl)O, 1600 $\nu(OCO)_{asym}$. ^{119}Sn Mössbauer data: δ = 1.47, Δ = 3.85, $\Gamma\pm$ = 0.82 mm s^{-1}, calculated C–Sn–C = 156° (X-ray: 150.4(1)).

*2.4.2.4. Synthesis of [^{n}Bu$_2$Sn(L^1)(L^5)]$_2$ (**5**).* Orange crystals of **5** were obtained from ethanol–acetone (v/v 1:1). Yield: 0.39 g (40.6%), M.p. 161–162 °C. Anal. Calc. for $C_{88}H_{86}$ $Cl_2N_{12}O_{10}Sn_2$: C, 59.38; H, 4.87; N, 9.44. Found: C, 60.01; H, 4.57; N, 9.46%. IR (KBr, cm^{-1}): 1248 ν(C(aryl)O, 1613 $\nu(OCO)_{asym}$. ^{119}Sn Mössbauer data: δ = 1.50, Δ = 4.17, $\Gamma\pm$ = 0.79 mm s^{-1}, calculated C–Sn–C = 180° (X-ray: 168.1(1)).

*2.4.2.5. Synthesis of [^{n}Bu$_2$Sn(L^1)(L^6)]$_2$ (**6**).* Orange crystals of **6** were obtained from benzene–cyclohexane (v/v 1:2). Yield: 0.50 g (59.5%), M.p. 130–132 °C. Anal. Calc. for $C_{76}H_{78}N_{10}O_{12}Sn_2$: C, 58.48; H, 5.04; N, 8.97. Found: C, 58.50; H, 4.87; N, 8.76%. IR (KBr, cm^{-1}): 1255 ν(C(aryl)O, 1653 $\nu(OCO)_{asym}$. ^{119}Sn Mössbauer data: δ = 1.40, Δ = 3.60, $\Gamma\pm$ = 0.78 mm s^{-1}, calculated C–Sn–C = 146° (X-ray: 156.8(1) for molecule A and 147.7(2) for molecule B; average C–Sn–C bond angle 152.2°).

2.5. X-ray crystallography

Crystals of **1**–**6** suitable for X-ray crystal-structure determination were obtained from benzene/hexane (**1** and **3**), chloroform/cyclohexane (**2**), toluene/chloroform (**4**), ethanol/acetone (**5**) and benzene/cyclohexane (**6**) solutions of the respective compounds. All measurements were made at 160 K on a Nonius Kappa-CCD diffractometer [20] with graphite-monochromated Mo Kα radiation (λ = 0.71073 Å) and an Oxford Cryosystems Cryostream 700 cooler. Data reduction was performed with HKL Denzo and Scalepack [21]. The intensities were corrected for *Lorentz* and polarization effects, and an empirical absorption correction based on the multi-scan method [22] was applied. A summary of crystal data, data collection and structure refinement parameters are given in Table 1. The structures were solved by direct methods using SIR92 [23] or SHELXS97 [24] and refined against F^2 for all reflections using the SHELXL97 [25] software.

The Sn-complexes **2**–**6** are centrosymmetric dinuclear molecules with one half of the molecule in the asymmetric unit. In **6**, the asymmetric unit contains one half of each of two centrosymmetric molecules. The atomic coordinates of the two molecules were tested carefully for a relationship from a higher symmetry space group using the program PLATON [26], but none was found.

The structure of **2** also contains cyclohexane molecules which are located about threefold inversion centres, giving a solvent:complex ratio of 1:3. The terminal methoxyphenyl group of the azo ligand in **2** is disordered, while one of the *n*-butyl groups is disordered in one of the independent molecules of **4** and in **6**. The disorder was modelled in each case by defining two positions for each disordered atom, refining an overall site occupation factor for each conformation and applying similarity restraints to the chemically equivalent bond lengths and angles involving all disordered atoms, while neighbouring atoms within and between each conformation of the disordered group were restrained to have similar atomic displacement parameters. The non-hydrogen atoms were refined anisotropically. The hydroxy H-atoms were placed in the positions indicated by a difference electron density map and their positions were allowed to refine together with individual isotropic displacement parameters. All other H-atoms were placed in geometrically calculated positions and refined using a riding model where each H-atom was assigned a fixed isotropic displacement parameter with a value equal to 1.2 U_{eq} of its parent atom (1.5 U_{eq} for the methyl groups).

3. Results and discussion

3.1. Preparation and characterization

The mixed ligand di-*n*-butyltin(IV) complexes (**2**–**6**) were obtained from equimolar reactions of **1**, prepared as described previously [5], with the appropriate substituted benzoic acid in refluxing toluene, in the presence of Et_3N, in 40–68% yield. All the compounds have well-defined melting points, are stable in the air and soluble in common organic solvents. The analytical data defined the metal-to-ligand ratio which supported the formulations of the products (see Section 2).

Table 1
Crystallographic data and structure refinement parameters for di-*n*-butyltin(IV) compounds **1**–**6**.

	1	**2**	**3**	**4**	**5**	**6**
Empirical formula	$C_{24}H_{30}ClN_3O_2Sn$	$C_{62}H_{70}N_6O_8Sn_2 \cdot 0.33C_6H_{12}$	$C_{76}H_{82}N_{10}O_{10}Sn_2$	$C_{76}H_{82}N_{10}O_{10}Sn_2$	$C_{88}H_{86}Cl_2N_{12}O_{10}Sn_2$	$C_{76}H_{78}N_{10}O_{12}Sn_2$
Molecular weight	546.57	1292.52	1532.74	1532.74	1779.82	1560.71
Crystal size (mm)	0.05 × 0.17 × 0.28	0.18 × 0.20 × 0.25	0.05 × 0.15 × 0.23	0.10 × 0.15 × 0.25	0.15 × 0.22 × 0.32	0.25 × 0.25 × 0.35
Crystal system	Triclinic	Trigonal	Triclinic	Triclinic	Monoclinic	Triclinic
Space group	$P\bar{1}$	$R\bar{3}$	$P\bar{1}$	$P\bar{1}$	$P2_1/c$	$P\bar{1}$
a (Å)	7.1363(1)	34.5459(3)	10.2516(3)	10.3634(2)	10.8834(1)	12.2249(3)
b (Å)	7.8377(1)	34.5459(3)	13.6965(5)	10.7030(2)	20.8341(2)	12.2740(2)
c (Å)	21.8378(4)	12.9981(1)	13.7049(5)	17.0291(4)	18.3434(2)	25.2903(4)
α (°)	79.9572(9)	90	65.084(2)	100.164(1)	90	97.105(1)
β (°)	85.616(1)	90	89.347(2)	100.587(1)	106.5608(7)	94.069(1)
γ (°)	83.558(1)	120	87.401(2)	104.604(1)	90	107.000(1)
V (Å^3)	1193.11(3)	13433.9(2)	1743.4(1)	1746.74(6)	3986.75(7)	3578.1(1)
Z	2	9	1	1	2	2
D_x (g cm^{-3})	1.521	1.438	1.460	1.457	1.483	1.448
μ (mm^{-1})	1.207	0.896	0.783	0.782	0.762	0.767
Transmission factors (minimum/maximum)	0.822, 0.947	0.784, 0.866	0.896, 0.962	0.626, 0.945	0.810, 0.893	0.748, 0.826
$2\theta_{max}$ (°)	60	60	55	60	60	60
Reflections measured	30870	76280	40005	47144	95357	61859
Independent reflections/R_{int}	6915/0.053	8733/0.081	7969/0.072	10207/0.088	11645/0.074	20626/0.065
Independent reflections with $I > 2\sigma(I)$	6171	6505	6554	8372	8940	14549
Number of parameters/restraints	283/0	439/246	451/0	479/52	521/0	954/123
$R(F)$ ($I > 2\sigma(I)$ reflections)	0.0333	0.0406	0.0415	0.0489	0.0441	0.0457
$wR(F^2)$ (all data)	0.0814	0.1060	0.0978	0.1303	0.1155	0.1202
Goodness-of-fit (F^2)	1.108	1.092	1.097	1.042	1.077	1.047
Maximum, minimum $\Delta\rho$ (e/Å^3)	1.16, −1.35	2.38, −1.08	1.15, −1.35	0.92, −1.06	0.91, −0.87	1.68, −0.99

Based on the data obtained previously for **1** [5], a distorted trigonal bipyramidal geometry has been proposed for the tin atom, with the Cl- and N-atoms in the axial positions. Its strong IR band at 1259 cm^{-1}, assigned to the *ν(C(aryl)-O)*, i.e. C_8–O–Sn linkage in the complex **1** does not shift appreciably upon complexation with the benzoates [5] (**2**–**6**, see Section 2). By contrast, the infrared band associated with the antisymmetric [ν_{asym}(OCO)] stretching shows a substantial shift (50–110 cm^{-1}) in mixed ligand complexes **2**–**6**, when compared with the respective benzoic acids (L^2H': 1693, L^3H': 1701, L^4H': 1653, L^5H': 1725, L^6H': 1733 cm^{-1}). The shift of the [ν_{asym}(OCO)] band to lower wave number is ascribed to carboxylate coordination, as reported earlier [17–19], supporting the formulation of the mixed ligand complexes.

3.2. Crystal structures

Scheme 2 depicts the chemical structures of complexes **1**–**6**. The presence of solvent in the structure of **2** and disorder in **2**, **4** and **6** is discussed in Section 2.5. Compound **1** is a mononuclear complex in which the tin atom is five-coordinate (Fig. 1). The coordination geometry is best described as distorted *cis*-trigonal bipyramidal. The bidentate quinolin-8-olate ligand coordinates such that the N- and O-atoms are in axial and equatorial positions, respectively. The other axial position is occupied by the Cl-atom and the *n*-butyl groups complete the equatorial plane. The distortions from perfect trigonal bipyramidal geometry cause an opening of the C–Sn–C angle and a deviation of the axial Cl–Sn–N bond angle by ca. 20° from linearity and in a direction that allows the axial atoms to release steric strain from the *n*-butyl groups (Table 2). The five-membered chelate ring has a slight envelope puckering with the tin atom lying 0.3294(1) Å from the plane of the other four atoms. The steric strain in the small chelate ring is manifested in the significantly distorted bond angles at N(1); much more so than at C(1).

The structure of the corresponding diethyl analogue of **1** has been reported [27]. That compound is a one-dimensional zig-zag *cis*-Cl-bridged polymer resulting from an additional long intermolecular Sn–Cl contact of 3.69 Å, which completes a distorted octahedral coordination sphere about each tin atom. It would seem that the bulk of the *n*-butyl groups in **1** blocks the approach of another atom from a second molecule and thereby precludes the formation of a similar polymeric structure. In all other respects, the geometric parameters and distortions involving the bidentate quinolin-8-olate ligand in the di-*n*-butyl and diethyl derivatives are very similar. The Cambridge Structural Database (CSD; version 4.29 with January 2008 updates) [28] contains atomic coordinate data for just 20 quinolin-8-olato-Sn(IV) complexes which do not contain another metal. Of these, 18 have six-coordinate tin atoms and 17 are bis(quinolin-8-olate) complexes. The Sn–N bond lengths range from 2.20 to 2.60 Å, mean 2.35 Å, with most entries lying in the range 2.30–2.43 Å. The Sn–O bond lengths range from 2.03 to 2.12 Å, mean 2.09 Å, and the intraring C–N–Sn angle is in the range 107.4–113.3°, mean 110.6°. The corresponding parameters for **1** lie well within these ranges and, except for the somewhat shorter Sn–O bond, close to the mean values.

The molecular structures of complexes **2**–**5** are centrosymmetric dinuclear Sn-complexes in which the monomeric [^{n}Bu$_2$Sn(L^1)-(L^x)] entity found in solution (see the following discussion of the solution ^{117}Sn NMR) has dimerized *via* two symmetry-equivalent, but highly asymmetric μ-O bridges involving the quinolin-8-olate O-atom to give a cyclic Sn_2O_2 core (Figs. 2–5). The shorter Sn(1)–O(1) bonds in the bridge range from 2.176(2) Å in **4** to 2.275(2) Å in **5**, while the longer Sn(1′)–O(1) bonds range from 2.555(2) Å in **5** to 2.678(2) Å in **2**, giving a difference in these distances of 0.40–0.48 Å for **2**–**4** and 0.28 Å for **5** (Table 3). The most symmetric bridges are found in **5**. Essentially, the two longer Sn(1')–O(1) interactions provide weak links between the formal monomeric units and explain the absence of significant quantities of the dinuclear species in solution. The Sn···Sn distances within the Sn_2O_2 cores of **2**–**5** are 4.1035(3), 4.0660(3), 4.0695(3) and 3.9723(2) Å, respectively.

Each tin atom is coordinated by the bidentate quinolin-8-olate ligand, the longer bridging interaction from the centrosymmetrically-related quinolin-8-olate O-atom, the two *n*-butyl groups and by the carboxylate O-atoms of the benzoate ligand. In complexes **2**–**4**, the benzoate ligand O-atoms coordinate highly asymmetrically to the tin atom with the distance to the carboxylate

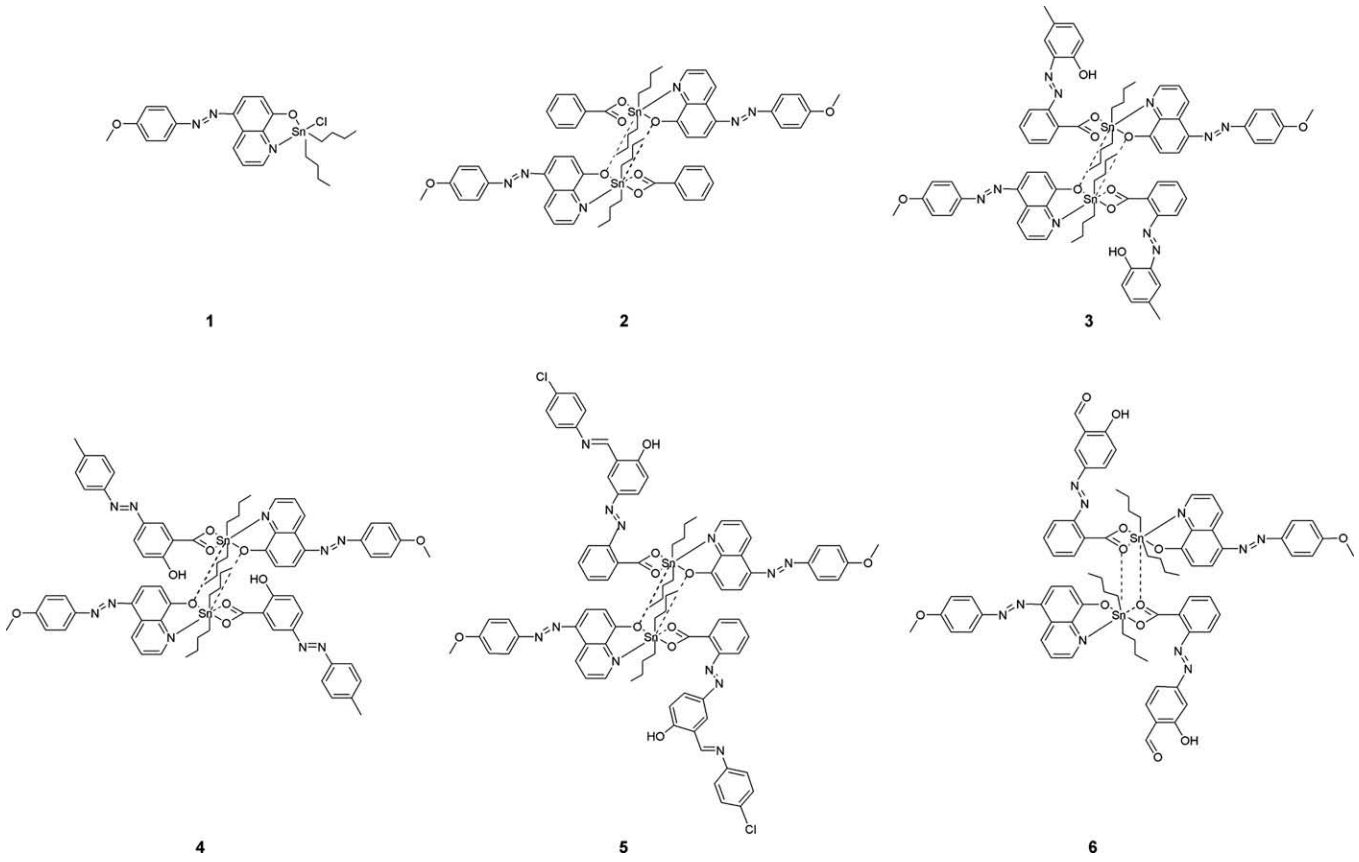

Scheme 2. Schematic representation of the structures of the complexes **1**–**6**.

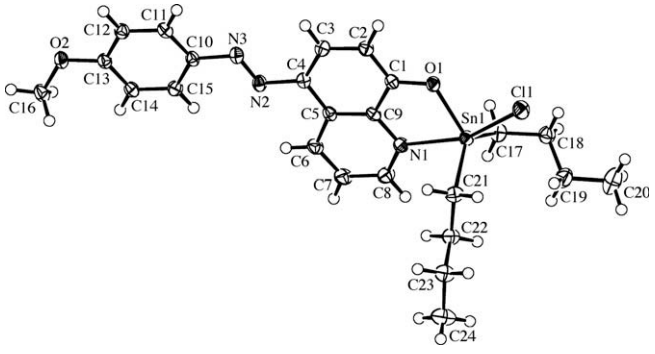

Fig. 1. The molecular structure of $^{n}Bu_2SnCl(L^1)$ (**1**). Displacement ellipsoids are shown at the 50% probability level.

Table 2
Selected interatomic distances (Å) and angles (°) for compound **1**.

Sn(1)–O(1)	2.044(2)
Sn(1)–N(1)	2.364(2)
Sn(1)–Cl(1)	2.4514(6)
Sn(1)–C(17)	2.139(2)
Sn(1)–C(21)	2.137(2)
O(1)–C(1)	1.339(3)
N(1)–C(8)	1.328(3)
N(1)–C(9)	1.364(3)
O(1)–Sn(1)–C(17)	111.06(8)
O(1)–Sn(1)–C(21)	118.38(8)
C(17)–Sn(1)–C(21)	128.8(1)
O(1)–Sn(1)–N(1)	74.51(6)
C(17)–Sn(1)–N(1)	89.03(8)
C(21)–Sn(1)–N(1)	91.83(8)
O(1)–Sn(1)–Cl(1)	85.55(5)
C(17)–Sn(1)–Cl(1)	101.47(7)
C(21)–Sn(1)–Cl(1)	94.79(7)
N(1)–Sn(1)–Cl(1)	159.79(5)
C(1)–O(1)–Sn(1)	119.3(1)
C(8)–N(1)–Sn(1)	131.6(2)
C(9)–N(1)–Sn(1)	109.3(1)

carbonyl O-atom, Sn(1)–O(3), lying in the range 2.915(2)–3.030(2) Å and the shorter Sn(1)–O(2) distance in the range 2.218(2)–2.247(2) Å (Table 3). When all interactions are considered, the coordination geometry about each tin atom may be described as a distorted pentagonal bipyramid where the *n*-butyl groups occupy the axial positions. The equatorially coordinated atoms, the tin atoms and the entire quinolin-8-olate moiety form a highly planar system. The main deviations from pentagonal bipyramid geometry arise from the bite angles of the three chelating rings in the complex plus the significant deviation from linearity of the C–Sn–C angles involving the *n*-butyl groups by 26–30°. This latter distortion bends the *n*-butyl groups slightly away from the quinolin-8-olate ligand. If one was to consider the very long Sn(1)–O(3) distance as being an insignificant, or at least a very weak interaction, the coordination environment might be described as distorted octahedral, and this is consistent with the solid-state ^{117}Sn NMR data, as discussed in more detail later. Nonetheless, the steric constraints enforced by the coplanar coordination of the benzoate and quinolin-8-olate ligands to the tin atom mean that atom O(3) has a significant influence on the overall distribution of the ligands about the metal centre.

The molecular structure of complex **5** is essentially the same as those of **2**–**4**, but the μ-O bridge is more symmetric and the benzo-

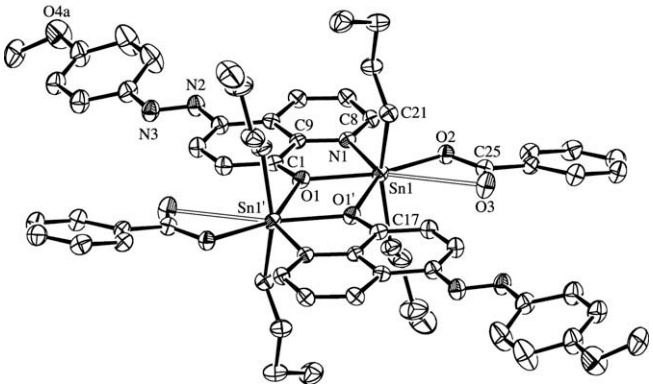

Fig. 2. The molecular structure of $[^nBu_2Sn(L^1)(L^2)]_2$ (**2**). Displacement ellipsoids are shown at the 40% probability level. H-atoms are omitted for clarity. Only one orientation of the disordered terminal methoxyphenyl group is shown.

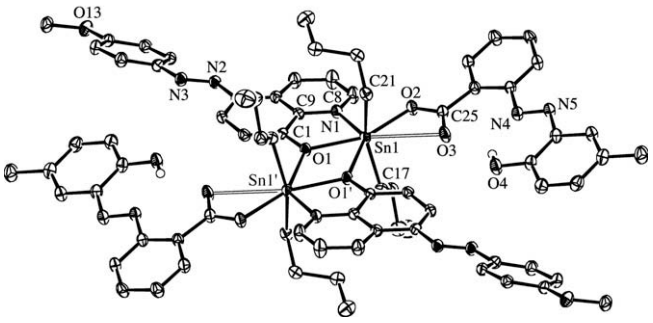

Fig. 3. The molecular structure of $[^nBu_2Sn(L^1)(L^3)]_2$ (**3**). Displacement ellipsoids are shown at the 40% probability level. Most H-atoms are omitted for clarity.

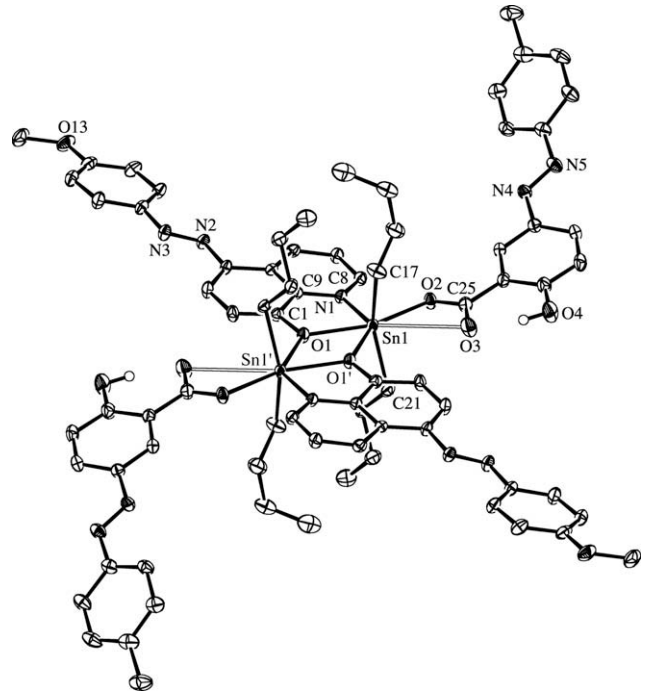

Fig. 4. The molecular structure of $[^nBu_2Sn(L^1)(L^4)]_2$ (**4**). Displacement ellipsoids are shown at the 40% probability level. Most H-atoms are omitted for clarity. Only one orientation of the disordered *n*-butyl groups is shown.

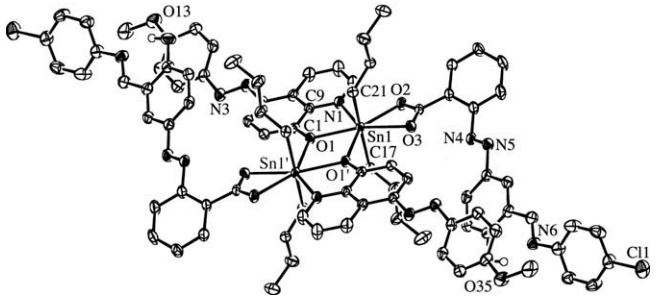

Fig. 5. The molecular structure of $[^nBu_2Sn(L^1)(L^5)]_2$ (**5**). Displacement ellipsoids are shown at the 50% probability level. Most H-atoms are omitted for clarity.

Table 3
Selected interatomic distances (Å) and angles (°) for compounds **2**–**5**.

Bond length or angle[a]	2	3	4	5
Sn(1)–O(1)	2.201(2)	2.202(2)	2.176(2)	2.275(2)
O(1)–Sn(1′)	2.678(2)	2.610(2)	2.647(2)	2.555(2)
Sn(1)–O(2) [**Sn–O–C**=O]	2.218(2)	2.232(2)	2.247(2)	2.327(2)
Sn(1)–O(3) [**Sn–O**=**C**–O]	2.976(2)	2.915(2)	3.030(2)	2.441(2)
Sn(1)–N(1)	2.259(2)	2.278(2)	2.256(2)	2.323(2)
Sn(1)–C(17)	2.116(3)	2.120(3)	2.115(3)	2.126(3)
Sn(1)–C(21)	2.117(3)	2.132(3)	2.119(3)	2.129(3)
O(1)–C(1)	1.317(3)	1.318(3)	1.334(3)	1.330(3)
O(2)–C(25)	1.274(3)	1.291(3)	1.277(4)	1.267(3)
O(3)–C(25)	1.238(3)	1.235(3)	1.252(4)	1.250(3)
N(1)–C(8)	1.329(3)	1.329(4)	1.332(4)	1.329(3)
N(1)–C(9)	1.371(3)	1.369(3)	1.370(3)	1.373(3)
C(17)–Sn(1)–C(21)	152.0(1)	153.6(1)	150.4(1)	168.1(1)
C(17)–Sn(1)–O(1)	95.21(9)	96.38(9)	96.1(1)	90.19(8)
C(21)–Sn(1)–O(1)	96.05(9)	96.15(9)	96.4(1)	91.51(8)
C(17)–Sn(1)–O(2)	89.80(9)	92.66(9)	89.6(1)	90.90(9)
C(21)–Sn(1)–O(2)	92.24(9)	87.79(9)	91.6(1)	93.64(8)
O(1)–Sn(1)–O(2)	151.82(6)	150.31(7)	152.43(8)	149.17(6)
C(17)–Sn(1)–N(1)	105.4(1)	100.7(1)	101.9(1)	95.83(9)
C(21)–Sn(1)–N(1)	102.36(9)	105.2(1)	107.4(1)	95.87(9)
O(1)–Sn(1)–N(1)	73.41(7)	72.91(7)	73.80(8)	71.92(7)
O(2)–Sn(1)–N(1)	78.51(7)	77.65(7)	78.63(8)	77.32(7)
C(17)–Sn(1)–O(1′)	79.74(8)	81.76(9)	79.5(1)	86.22(8)
C(21)–Sn(1)–O(1′)	81.65(8)	82.72(9)	81.5(1)	83.38(8)
O(1)–Sn(1)–O(1′)	65.85(6)	64.93(7)	65.28(8)	69.47(6)
O(2)–Sn(1)–O(1′)	142.22(6)	144.61(6)	142.21(7)	141.33(6)
N(1)–Sn(1)–O(1′)	139.25(6)	137.74(7)	138.91(7)	141.35(6)
Sn(1)–O(1)–Sn(1′)	114.15(6)	115.07(7)	114.72(8)	110.53(6)

[a] Primed atoms are moved through the molecular centre of inversion by the symmetry operator $1-x, -y, 1-z$ for **2** and **4**, $1-x, -y, 2-z$ for **3**, and $-x, -y, 2-z$ for **5**.

ate ligand coordinates almost symmetrically to the tin atom with the Sn(1)–O(3) distance now being much shorter at 2.441(2)° (Table 3). In this case, the tin atom is formally seven-coordinate and a more regular pentagonal bipyramidal geometry results, in which the deviation of the C–Sn–C angle from linearity is only 11.9(1)°.

The five-membered chelate ring involving the quinolin-8-olate moiety has a slight envelope conformation puckered on the tin atom in the structure of **4**, but is virtually planar in the other structures. The Sn–O bond lengths involving the quinolin-8-olate moiety are about 0.10–0.15 Å longer in **2**–**4** than in **1** and in the related quinolin-8-olate structures in the CSD and as much as 0.23 Å longer in **5** than in **1**. The Sn–N bond lengths are correspondingly shorter than in **1** and related structures, although the difference is much smaller in **5**. Unlike in **1**, the bond angles at N(1) do not show significant distortion in any of complexes **2**–**5**.

Dinuclear Sn-complexes involving the quinolin-8-olate ligand have not been reported previously. The CSD contains data for 124 dinuclear Sn(IV) structures with an Sn_2O_2 core and the bridging O-atom bonded to a C-atom. Over 80% of these structures have centrosymmetric cores. There is a cluster of 40 structures with

almost perfectly symmetrical μ-O bridges having a difference between the longer and shorter of the Sn–O bonds of less than 0.04 Å and another 13 up to a difference of 0.10 Å. There are 66 structures with their bond length difference scattered fairly evenly over the range of 0.10–0.44 Å, with five structures in the 0.45–0.64 Å range. Thus, the observed asymmetry of the μ-O bridges in **2**–**5** is consistent with other observations, but the differences in the bridging Sn–O bond lengths of 0.40–0.48 Å in the cases of **2**–**4** tend toward the upper end of the observed range. The absolute values of the Sn–O bond lengths in these literature structures vary widely from 2.0 to 2.9 Å and are clearly related to the coordination environment and nature of the ligands involved, so a direct comparison with the current structures is less enlightening. However, there is a tendency for the Sn–O bonds on each side of the O-atom to be either both quite long (>2.3 Å) or both much shorter (2.0–2.3 Å), with relatively few examples of one very long and one very short bond.

The molecule of **6** is also a centrosymmetric dinuclear Sn-complex, but the core motif is different. Instead of the μ-O bridges *via* the quinolin-8-olate O-atom observed in **2**–**5**, the carboxylate groups of two benzoate ligands bridge the two tin atoms to give a cyclic $Sn_2C_2O_4$ core motif (Fig. 6). Each tin atom in **6** is coordinated by a bidentate quinolin-8-olate ligand, two O-atoms from the two carboxylate bridges and two *n*-butyl groups. This results in a distorted octahedral coordination geometry about each tin atom with the *n*-butyl groups in the *trans* positions. The asymmetric unit of the crystal structure of **6** contains one half of each of two molecules, where these molecules sit across crystallographic centres of inversion. Most of the geometric parameters of the two independent molecules are quite similar, with the major differences being in the conformation of one *n*-butyl group and in the length of the longer of the bridging Sn–O bonds which differs by about 0.12 Å (Table 4). The solid-state ^{117}Sn NMR measurements also detect two distinct structures, as discussed later. Once again, the bridges are quite asymmetric, with the Sn–O bond lengths in the bridge differing by 0.51 and 0.64 Å in molecules A and B, respectively. The longer Sn–O distance involves the carboxylate carbonyl O-atom in each molecule. Despite the bridge in **6** being a carboxylate group, the short and long Sn–O bonds in the bridge are very similar in length to those involving the μ-O-atom in complexes **2**–**5**. However, the distances between the tin atom and the carboxylate carbonyl O-atom of 2.683(2) and 2.798(2) Å for molecules A and B, respectively, are now significantly shorter than the corresponding long distances of 2.92–3.03 Å in complexes **2**–**4**. The Sn···Sn distance within the core of **6** is 4.6165(3) and 4.6831(3) Å for molecule A and B, respectively, which reflects the additional spacing between these atoms introduced by the three-atom carboxylate bridge when compared with the single-atom μ-O bridges in **2**–**5**. Now that the quinolin-8-olate O-atom is not involved in a bridge in **6**, the quinolin-8-olate Sn–O bond is 0.1–0.2 Å shorter than in the other dinuclear complexes, but comparable with that in **1**. The Sn–N bonds are also more similar to that in **1** than in the other dinuclear complexes, which are shorter. The carboxylate carbonyl O-atom is also within a contact distance of the tin atom to which carboxylate group is primarily coordinated, with these Sn···O distances being 3.085(2) and 2.898(2) Å for molecules A and B, respectively. If all interactions with the tin atoms are considered, as in **2**–**5**, the geometric arrangement about each tin atom in **6** is a distorted pentagonal bipyramid with the *n*-butyl groups in the axial positions.

The CSD records data for 26 structures containing an $Sn_2C_2O_4$ core involving bridging carboxylate ligands. Ten of these are dinuclear Sn(IV) complexes, of which nine have centrosymmetric cores and most have reasonably symmetric Sn–O distances in the bridges in which the longest Sn–O distance is less than 2.35 Å. The only dinuclear Sn(IV) structure with asymmetric bridge dimensions similar to those in **6** is bis(tetrakis(triphenylphosphine-P)-silver(I)) bis(μ_2-trifluoroacetato-O,O')-tetrakis(trifluoroacetato-O)-tetramethyl-di-tin(IV) [29], where the longer Sn–O distance is 2.82 Å.

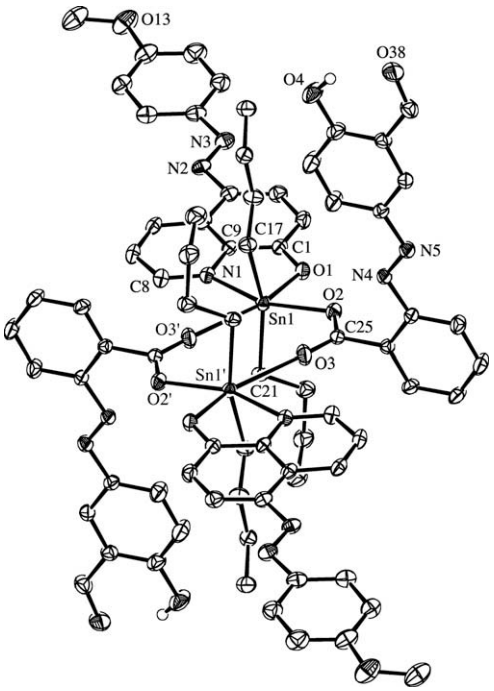

Fig. 6. The molecular structure of one of the two symmetry-independent molecules of [^{n}Bu$_2$Sn(L^1)(L^6)]$_2$ (**6**). Displacement ellipsoids are shown at the 40% probability level. Most H-atoms are omitted for clarity.

Table 4
Selected interatomic distances (Å) and angles (°) for the two symmetry-independent molecules of **6**.

Bond length or angle[a]	Molecule A	Bond length or angle	Molecule B
Sn(1)–O(1)	2.086(2)	Sn(2)–O(5)	2.083(2)
Sn(1)–O(2) [**Sn–O–C=O**]	2.171(2)	Sn(2)–O(6)	2.167(2)
O(3)–Sn(1') [**Sn–O=C–O**]	2.683(2)	Sn(2)–O(7″)	2.798(2)
Sn(1)–O(3)	3.085(2)	Sn(2)–O(7)	2.898(2)
Sn(1)–N(1)	2.345(2)	Sn(2)–N(8)	2.343(2)
Sn(1)–C(17)	2.133(3)	Sn(2)–C(57)	2.121(3)
Sn(1)–C(21)	2.120(3)	Sn(2)–C(61a)	2.119(4)
O(1)–C(1)	1.321(3)	O(5)–C(41)	1.328(3)
O(2)–C(25)	1.282(3)	O(6)–C(65)	1.266(3)
O(3)–C(25)	1.227(3)	O(7)–C(65)	1.225(4)
N(1)–C(8)	1.319(4)	N(8)–C(48)	1.317(4)
N(1)–C(9)	1.361(3)	N(8)–C(49)	1.360(4)
O(1)–Sn(1)–C(21)	101.4(1)	O(5)–Sn(2)–C(61a)	107.0(2)
O(1)–Sn(1)–C(17)	101.7(1)	O(5)–Sn(2)–C(57)	103.4(1)
C(21)–Sn(1)–C(17)	156.8(1)	C(61a)–Sn(2)–C(57)	147.7(2)
O(1)–Sn(1)–O(2)	79.87(8)	O(5)–Sn(2)–O(6)	80.40(8)
C(21)–Sn(1)–O(2)	93.3(1)	C(61a)–Sn(2)–O(6)	99.4(3)
C(17)–Sn(1)–O(2)	93.2(1)	C(57)–Sn(2)–O(6)	96.1(1)
O(1)–Sn(1)–N(1)	74.68(8)	O(5)–Sn(2)–N(8)	74.39(8)
C(21)–Sn(1)–N(1)	94.1(1)	C(61a)–Sn(2)–N(8)	87.1(3)
C(17)–Sn(1)–N(1)	89.7(1)	C(57)–Sn(2)–N(8)	90.8(1)
O(2)–Sn(1)–N(1)	154.44(8)	O(6)–Sn(2)–N(8)	154.77(9)
O(1)–Sn(1)–O(3′)	160.27(7)	O(5)–Sn(2)–O(7″)	161.66(8)
C(21)–Sn(1)–O(3′)	77.37(9)	C(61a)–Sn(2)–O(7″)	71.8(2)
C(17)–Sn(1)–O(3′)	80.03(9)	C(57)–Sn(2)–O(7″)	75.9(1)
O(2)–Sn(1)–O(3′)	119.79(7)	O(6)–Sn(2)–O(7″)	117.93(7)
C(25)–O(3)–Sn(1′)	177.5(2)	C(65)–O(7)–Sn(2″)	171.6(2)

[a] Primed atoms are moved through the molecular centre of inversion by the symmetry operator $-x$, $1-y$, $1-z$ for molecule A and $-x$, $-y$, $-z$ for molecule B.

The hydroxy group in each carboxylate ligand in **3**–**6** forms an intraligand hydrogen bond with the nearest adjacent heteroatom, thereby completing a six-membered loop. In **3**, the hydroxy H-atom is involved in a bifurcated interaction with the second acceptor being the carboxylate carbonyl O-atom of the same ligand. In **2–5**, a very short intramolecular C(8)–H···O(2) interaction (H···O distances and C–H···O angles in the ranges 2.24–2.29 Å and 118–123°, respectively) consistently appears between the quinolin-8-

Table 5
^{1}H and ^{13}C NMR data[a] of compounds **2–6** in $CDCl_3$ solution.

Compound[a]	**2**		**3**		**4**		**5**		**6**	
Atom	$\delta(^{13}C)$	$\delta(^{1}H)$	$\delta(^{13}C)$	$\delta(^{1}H)$	$\delta(^{13}C)$	$\delta(^{1}H)$	$\delta(^{13}C)$	$\delta(^{1}H)$	$\delta(^{13}C)$	$\delta(^{1}H)$
2	144.8[c]	8.80[c]	145.2[c]	8.77[c]	145.2[c]	8.90[c]	145.5[c]	8.76[c]	145.0[c]	8.78[c]
3	122.2	7.66[c]	122.1	7.5[b]	122.3	7.7 [b]	122.1	7.5 [b]	122.1	7.5 [b]
4	136.7[c]	9.48[c]	136.8[c]	9.46[c] (d, 8.3)	137.5[c]	9.55[c] (d, 8.3)	137.0[c]	9.44[c] (d, 7.4)	137.0[c]	9.48[c]
4a	128.4	–	128.4		128.4		128.4		128.4	
5	136.4	–	136.3		136.6		136.2		136.3	
6	118.0	8.14 (d, 8.6)	118.0	8.11 (d, 8.7)	118.1	8.14 (d, 8.7)	118.1	8.03 (d, 8.7)	118.3	8.11 (d, 8.7)
7	115.0[c]	7.27 (d, 8.6)	114.8	7.23 (d, 8.7)	115.2[c]	7.27 (d, 8.7)	114.8[c]	7.13 (d, 8.7)	114.8[c]	7.19 (d, 8.7)
8	161.4	–	161.4		160.9		161.3		161.3	
8a	137[c]	–	137[c]		137[c]		137[c]		137[c]	
1′	147.6	–	147.6		147.6		147.6		147.6	
2′& 6′	124.3	7.90 (d, 8.9)	124.3	7.89 (d, 8.9)	124.4	7.90 (d, 8.9)	124.3	7.87 (d, 8.8)	124.3	7.88 (d, 8.7)
3′& 5′	114.2	6.98 (d, 8.9)	114.2	6.96 (d, 8.9)	114.3	6.97 (d, 8.9)	114.2	6.96 (d, 8.8)	114.2	6.96 (d, 8.7)
4′	161.4	–	161.4		161.6		161.5		161.4	
OCH_3	55.5	3.85	55.5	3.83	55.6	3.84	55.5	3.83	55.5	3.83
n-Bu (α)	26.4 [630/658]	1.52[c]	26.5 [619/643]	1.53[c]	26.6 [612/634]	1.53[c]	26.3 [618/650]	1.53[c]	26.3 [623/651]	1.52[c]
n-Bu (β)	26.9 [42]	1.64[c]	26.9 [38]	1.70[c]	27.2 [40]	1.69[c]	27.1 [34]	1.70[c]	27.0 [38]	1.67[c]
n-Bu (γ)	26.4 [102]	1.25[c]	26.3 [106]	1.24 (m)	26.4 [100/104]	1.26 (m)	26.5 [102]	1.21 (m)	26.4 [102]	1.23 (m)
n-Bu (δ)	13.5	0.73[c] (t, 7.0)	13.5	0.70 (t, 7.0)	13.8	0.73 (t, 7.2)	13.5	0.69 (t, 7.2)	13.5	0.70 (t, 7.2)
COO	174.6	–	174.0		175.6		173.9[c]		174.0[c]	
1″	131.8	–	129.9		115.2		131.4[c]		131.8[c]	
2″	130.2	8.12 (d, 7.0)	131.9	8.17 (dd, 7.5, 1.5)	164.1		130.6	7.97	130.8	7.98 (dd, 7.1, 1.8)
3″	128.1	7.40 (dd, 7.0, 7.3)	130.2	7.47 (td, 7.5, 1.5)	117.8	7.02 (d, 8.9)	131.5	7.43 (dd, 7.5, 1.5)	131.4	7.46 (td, 7.1, 1.8)
4″	132.3	7.51 (t, 7.3)	132.2	7.55 (td, 7.5, 1.5)	127.7	7.99 (dd, 8.9, 2.5)	129.9	7.49 (dd, 7.5, 1.5)	130.4	7.52 (td, 7.1, 1.8)
5″	128.1	7.40 (dd, 7.0, 7.3)	115.6	7.86 (d, 7.5)	145.2		116.7	7.59 (d, 7.5)	116.7	7.59 (dd, 7.1, 1.8)
6″	130.2	8.12 (d, 7.0)	149.4		127.9	8.60 (d, 2.5)	151.4		151.2	
7″	–	–	137.9		150.8		145.8		146.1	
8″	–	–	150.5		122.6	7.75 (d, 8.2)	129.0	7.96	130.8	8.09 (dd, 8.9, 2.5)
9″	–	–	118.4	6.83 (d, 8.6)	129.7	7.24 (d, 8.2)	118.0	7.01	118.5	6.99 (d, 8.9)
10″	–	–	134.5	7.08 (dd, 8.6, 1.5)	140.8		164.1		163.9	
11″	–	–	128.6		129.7	7.24 (d, 8.2)	118.7		120.2	
12″	–	–	133.1	7.69 (d 1.5)	122.6	7.75 (d, 8.2)	127.7	7.97 (d, 7.1)	130.0	8.16 (d, 2.5)
13″	–	–					162.2	8.47	196.3	9.88
14″	–	–					146.0			
15″ & 19″	–	–					122.2	7.00 (d, 8.4)		
16″ & 18″	–	–					129.5	7.20 (d, 8.4)		
17″	–	–					132.9			
ArOH	–	–		12.3[d]		12.09[d]		13.52		11.28
$ArCH_3$	–	–	20.3	2.44	21.4	2.37				

[a] For the ^{1}H and ^{13}C NMR assignments, refer to Scheme 1 for the numbering proposal of the ligand skeletons. Chemical shifts in ppm, multiplicity and coupling constants (in Hz) of ^{1}H resonances in parentheses. $^{13}C–^{117/119}Sn$ coupling constants (in Hz) between brackets.
[b] Resonance hidden under other resonances.
[c] Broadened.
[d] Very broad.

olate and carboxylate ligands coordinated to the same tin atom in the dinuclear molecule. In addition, an intramolecular C(2)–H···O(3) interaction between the quinolin-8-olate and carboxylate ligands coordinated to different tin atoms may be helping to stabilize the μ-O bridging mode in the dinuclear molecules. The H···O distances and C–H···O angles for this interaction are in the ranges 2.40–2.43 Å and 167–180°, respectively, for **2–4**, but for **5**, the H···O distance is extremely short at 2.09 Å (angle 159°). Interestingly, neither of these C–H···O interactions, nor any others, occur in the structure of **6**, which has a different mode of bridging between the tin atoms. It is therefore concluded that the C–H···O interactions are not the sole driving force controlling the bridging mode developed during the assembly of the dinuclear molecule. Other factors may be the steric arrangement necessary to accommodate the ligands about a tin atom or to efficiently pack the molecules in the crystal, given that the steric bulk of the carboxylate ligands is the main variable in these compounds.

3.3. Mössbauer data

The ^{119}Sn Mössbauer parameters for the di-*n*-butyltin(IV) mixed ligand complexes [^{n}Bu$_2$Sn(L^1)(L$^{2-6}$)]$_2$ (**2–6**) in the solid state are given in Section 2. Compared with the natural width, 0.65 mm s^{-1}, the spectra are characterized by narrow lines, which are in accordance with the presence of identical or very similar tin sites in the dimers. The isomer shifts, δ, are typical for tin(IV) atoms in organotin derivatives. The measured quadrupole splitting values, Δ, are consistent with the *trans*-R$_2$ octahedral structures which characterize the complexes **2–6**, albeit as severely distorted octahedra, if the longer of the intramolecular carboxylate Sn–O(3) interactions are ignored. The C–Sn–C bond angles may be evaluated by the literal point-charge model assuming that in octahedral R$_2$SnX$_4$ systems the quadrupole splitting Δ is set up just by the R$_2$Sn unit [30], being the partial quadrupole splitting (pqs) of the alkyl groups attached to tin(IV), [R], much larger than that of the other ligands. Under these approximations, $|\Delta| = -4[R](1-(3/4)\sin^2\theta)^{1/2}$, where θ is the C–Sn–C bond angle. Using the pqs [Alk] [15] = −1.03 mm s^{-1}, the C–Sn–C bond angles estimated for complexes **2–4** and **6**, (153°, 153°, 156°, 146°, see Section 2) agree quite well with the experimental values. As far as compound **5** is concerned, the Δ value, 4.17 mm s^{-1}, is typical of *trans*-R$_2$ octahedral structures with a linear C–Sn–C fragment. On the other hand, by using the same equation, the experimental value of the C–Sn–C bond angle, 168.1(1)°, would give a calculated Δ value of 4.05 mm s^{-1}, in ±0.1 mm s^{-1} error in comparison with the observed value, well within the ±0.4 mm s^{-1} range accepted by the point-charge method. Such a deviation may be due to a variation of the bonding nature of the ligands and to a more negative pqs of the alkyl group, as a consequence of the much shorter Sn–O(3) distance, which effectively increases the coordination number of the tin atom, and results in a chemical environment with a much more regular pentagonal bipyramidal geometry, and consequently a more linear C–Sn–C bond angle, compared with that in compounds **2–4** and **6**. This assumption is supported by the large Δ values observed for pentagonal bipyramidal complexes with C–Sn–C bond angles similar to that found in compound **5** [31]. However, the variations observed in the C–Sn–C bond angles determined from Mössbauer parameters and single crystal analysis by X-ray diffraction can not be put side by side owing to the dissimilar sampling techniques, for instance, bulk powder and single crystal, respectively.

3.4. Solution and solid-state ^{117}Sn NMR

Characterization of complexes **2–6** in a CDCl$_3$ solution (approx. 10 mg in 0.7 ml) was performed by ^{1}H, ^{13}C and ^{117}Sn NMR. A combination of 1D ^{1}H, ^{13}C (proton decoupled and DEPT) and 2D ^{1}H–^{13}C correlation spectra (HSQC and HMBC), assisted in some cases by ^{1}H–^{1}H COSY spectra, allowed complete assignment of all ^{1}H and ^{13}C resonances. These data are summarized in Table 5. Only one set of resonances is observed at room temperature, but some resonances are broad, suggesting some dynamic process might be operative in solution.

The solution ^{117}Sn spectrum at 303 K reveals three resonances for compounds **2**, **5** and **6**, two resonances for **3** and a single resonance for **4** (Table 6) with a chemical shift of −170 ppm. The major resonance of the compounds **2**, **3**, **5** and **6** has a chemical shift ranging from −185 to −188 ppm. Compounds **2**, **5** and **6** also display a smaller resonance between −143 and −150 ppm, while all (except **4**) also show the presence of a species with a chemical shift around −252 ppm. All these resonances are broad (between 200 and 700 Hz), especially the one around −185 ppm, supporting the previous assumption of a dynamic process being present in solution. The different chemical shifts reflect different modes of coordination of the tin atom, to be ascribed to complexes in which some bonds are broken, when compared to the tin coordination in the solid state (*vide infra*). In order to get some insight into this dynamic process and to characterize the nature of the different species in equilibrium, a more concentrated sample of **2** was subjected to a variable temperature study. Fig. 7a displays a selection of the ^{117}Sn spectra at low temperature. As the temperature is lowered, the resonance at −188 ppm sharpens and shifts slightly to lower frequency, while the resonance at −252 ppm diminishes in intensity and finally disappears into the noise while a new resonance appears at −100 ppm. At 233 K, most of the ^{1}H resonances are sharpened up when compared to 303 K, and additional small resonances appear (Fig. 7b). A ^{1}H–^{117}Sn correlation spectrum at 233 K reveals that the major tin resonance at −188 ppm correlates with the H-2 proton (at 8.80 ppm) of the quinolin-8-ol ligand, while the small resonance at −252 ppm correlates with the small new resonance at 8.52 ppm, which is assigned to the H-2 proton in a less abundant species. All these observations are rationalized

Table 6
Solution (CDCl$_3$) and solid-state ^{117}Sn NMR data for compounds **2–6**.

Compound	$\delta(^{117}Sn)$[a]	^{117}Sn MAS[b]					
		δ_{iso}	ζ	η	δ_{11}	δ_{22}	δ_{33}
2	−150.3 (230, 15%), −187.7 (450, 72%), −251.9 (190, 13%)	−268	−675	0.35	188	−48	−943
3	−187.9 (700, 95%), −251.8 (250, 5%)	−292	−705	0.40	202	−80	−997
4	−170.4 (375, 100%)	−258	−612	0.45	185	−90	−870
5	−145.9 (210, 8%), −186.1 (265, 80%), −251.1 (280, 12%)	−368	−714	0.00	−11	−11	−1082
6	−143.3 (360, 8%), −185.2 (430, 82%), −251.4 (250, 10%)	−245	−653	0.25	163	0	−897
		−261	−622	0.30	143	−43	−883

[a] In CDCl$_3$ solution. The numbers in parentheses are the widths at half height (in Hz) and the percentage amplitudes of the resonances.
[b] δ_{iso} (ppm) = $(\delta_{11} + \delta_{22} + \delta_{33})/3$; ζ(ppm) = $\delta_{33} - \delta_{iso}$ and $\eta = |\delta_{22} - \delta_{11}|/|\delta_{33} - \delta_{iso}|$ were δ_{11}, δ_{22} and δ_{33} (ppm) are the principal tensor components of the chemical shielding anisotropy, sorted as follows $|\delta_{33} - \delta_{iso}| > |\delta_{11} - \delta_{iso}| - |\delta_{22} - \delta_{iso}|$.

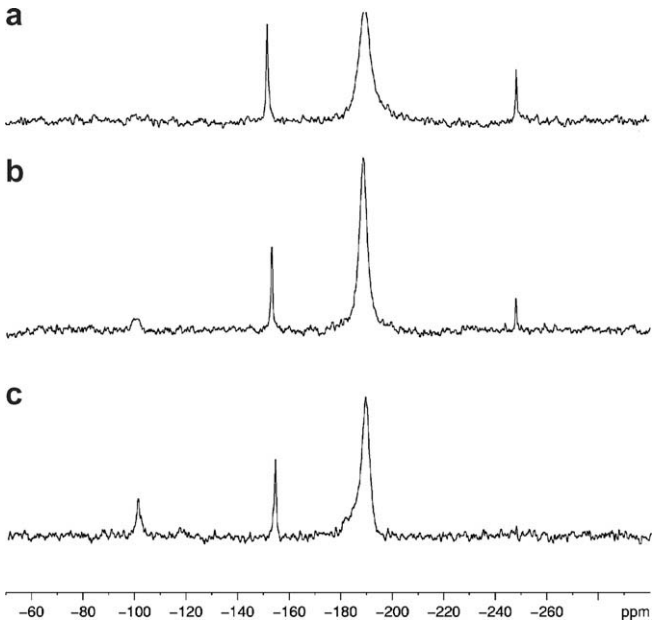

Fig. 7a. The ^{117}Sn NMR spectra of **2** in $CDCl_3$ from bottom to top (a) at 253 K, (b) at 233 K and (c) at 213 K.

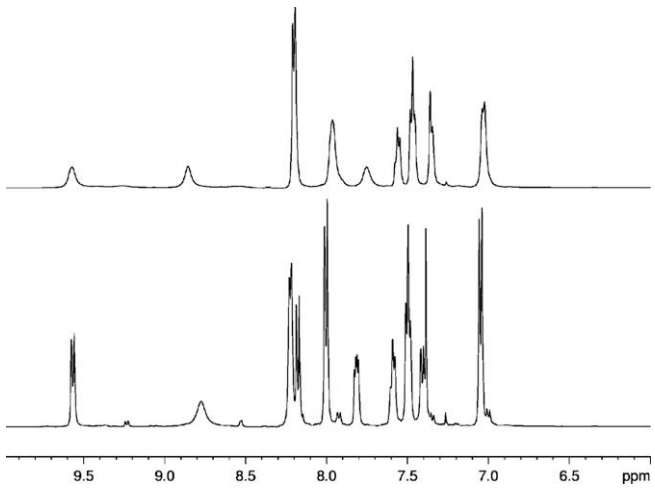

Fig. 7b. The aromatic region of the ^{1}H NMR spectra of **2** in $CDCl_3$ at 303 K (top) and 233 K (bottom).

as follows. In solution at room temperature, the major species consists of a six-coordinate monomeric species with the Sn-atom bound to the two *n*-butyl groups, chelated by the oxygen and nitrogen atoms of the quinolin-8-ol moiety as well as by both oxygen atoms of the carboxylate group. The resonance at −252 ppm is assigned to the dimeric species composed of the μ-O Sn_2O_2 core, involving the oxygen atom of the quinolin-8-ol moiety, as observed in the crystal structure. That this dimer does not appear as the dominant species in solution is quite acceptable, since, in spite of probable packing effects in the crystalline state, the Sn–O–Sn bridges giving rise to the dimers systematically contain one quite long Sn–O distance, and are thus not expected to be particularly strong. The resonance at −150 ppm is due to a structure in which the coordination with N-1 is lost, as demonstrated by the absence of correlation with the H-2 proton, and finally the resonance at −101 ppm, only visible at very low temperature (213 K), is assigned to a species in which the Sn←O=C–O– bond is also broken, leaving a four-coordinate species. The generation of a four-coordinate tin species at low temperature in solution may appear surprising at first glance, but is also acceptable in view of the expected reinforcement of the covalent Sn–O bond upon formation of a stronger monodentate carboxylate coordination at low temperature.

The solid-state ^{117}Sn NMR data (Table 6) are in agreement with the crystal structures. The isotropic chemical shifts for all compounds, except **5**, range roughly from −250 to −290 ppm, typical for six-coordination, thus reflecting the mostly rather loose seven-coordination of the tin atom in the dimeric species, as revealed by the crystal structures. The more negative chemical shift of compound **5** (−368 ppm) can be traced back to the ca. 0.47 Å shorter distance between the tin atom and the C=O(3) carboxylate oxygen atom than in the other compounds, as discussed earlier (Tables 3 and 4). The stronger coordination with this oxygen atom results in a low frequency shift while the principal tensor components are also affected. Compound **5** has axial symmetry (η = 0.0), while all others are nearly axially symmetric (η = 0.30–0.45). A special situation is encountered for compound **6**, since two isotropic chemical shifts can be discerned, with a distinctively different set of principal tensor components. One set is comparable to that of **2**–**4**, while the other set is somewhat different with a slightly higher frequency and a δ22 of 0, whereas the other compounds have δ22 values between −43 and −90 ppm. These solid-state NMR features can be correlated with the crystal structure of **6**, in which a different type of dimeric motif is observed, at least for the crystal analyzed. Unlike **2**, **3**, **4** and **5**, the $Sn_2C_2O_4$ core of **6**, as found from X-ray diffraction data, involves the carboxylate oxygen atoms instead of the quinolin-8-ol oxygen atom. The presence of two isotropic chemical shifts in the solid-state tin NMR spectrum of **6** is in agreement with the observation by X-ray diffraction where two molecules are present in the asymmetric unit (see Table 4). However, as solid-state NMR analyses the bulk sample, by contrast with single crystal analysis by X-ray diffraction, it could also be that compound **6** consists of constitutionally isomeric coordination motifs: the unique one found by X-ray diffraction, and another one in line with those of the other compounds, in particular **2** and **4**, in view of their more similar solid-state ^{117}Sn NMR data to those of **6**.

Thus, the NMR data altogether indicate that the different types of coordination are involved in a kind of dissociation–association competition depending in a complex way on crystal packing, the electronic and/or steric nature of the substituted benzoate ligand L^{2-6}, and, in solution, also on the temperature and the concentration; globally, however, it appears that intermolecular coordination giving rise to dimeric structures in the crystalline state are not the dominant factor, and occur with very versatile but weak coordination modalities, since the typical chemical shifts they give rise to in the crystalline state are not dominant in any of the complexes in solution.

Acknowledgements

The financial support of the Department of Science & Technology, New Delhi, India (Grant No. SR/S1/IC-03/2005, TSBB) and the University Grants Commission, New Delhi, India through SAP-DSA, Phase-III are gratefully acknowledged. M.B. and R.W. are indebted to the Fund for Scientific Research Flanders, Belgium (FWO) for financial support (Grant Nos. G.0064.07 and G.0469.06), as well as to the Research Council of the VUB for a Concerted Research Action funding (GOA31) as well as for various matching funds. G.R. is indebted to the Università di Palermo, Italy for financial support.

Appendix A. Supplementary material

CCDC 709235, 709236, 709237, 709238, 709239 and 709240 contains the supplementary crystallographic data for this paper. These data can be obtained free of charge from The Cambridge Crystallographic Data Centre via www.ccdc.cam.ac.uk/data_request/cif. Supplementary data associated with this article can be found, in the online version, at doi:10.1016/j.jorganchem.2009.02.021.

References

[1] E.O. Schlemper, Inorg. Chem. 6 (1967) 2012.
[2] W. Chen, W.K. Ng, V.G. Kumar Das, G.B. Jameson, R.J. Butcher, Acta Crystallogr. Sect. C 45 (1989) 861.
[3] E. Kellö, V. Vrábel, J. Holeček, J. Sivy, J. Organomet. Chem. 493 (1995) 13.
[4] A. Szorcsik, L. Nagy, M. Scopelliti, A. Deák, L. Pellerito, K. Hegetschweiler, J. Organomet. Chem. 690 (2005) 2243.
[5] T.S. Basu Baul, A. Mizar, A.K. Chandra, X. Song, G. Eng, R. Jirásko, M. Holčapek, D. de Vos, A. Linden, J. Inorg. Biochem. 102 (2008) 1719.
[6] A. Linden, T.S. Basu Baul, A. Mizar, Acta Crystallogr. Sect. E 61 (2005) m27.
[7] T.S. Basu Baul, A. Mizar, A. Lyčka, E. Rivarola, R. Jirásko, M. Holčapek, D. de Vos, U. Englert, J. Organomet. Chem. 691 (2006) 3416.
[8] T.S. Basu Baul, A. Mizar, X. Song, G. Eng, R. Willem, M. Biesemans, I. Verbruggen, R. Butcher, J. Organomet. Chem. 691 (2006) 2605.
[9] S.W. Ng, C. Wei, V.G. Kumar Das, J.P. Charland, F.E. Smith, J. Organomet. Chem. 364 (1989) 343.
[10] T.S. Basu Baul, E.R.T. Tiekink, J. Chem. Crystallogr. 26 (1996) 393.
[11] S.W. Ng, J. Organomet. Chem. 585 (1999) 12.
[12] T.S. Basu Baul, W. Rynjah, E. Rivarola, C. Pettinari, A. Linden, J. Organomet. Chem. 690 (2005) 1413.
[13] H.L. Xu, H.D. Yin, Z.J. Gao, G. Li, J. Organomet. Chem. 691 (2006) 3331.
[14] T.S. Basu Baul, A. Mizar, E. Rivarola, U. Englert, J. Organomet. Chem. 693 (2008) 1751.
[15] T.K. Sham, G.M. Bancroft, Inorg. Chem. 14 (1975) 2281.
[16] R. Willem, I. Verbruggen, M. Gielen, M. Biesemans, B. Mahieu, T.S. Basu Baul, E.R.T. Tiekink, Organometallics 17 (1998) 5758.
[17] T.S. Basu Baul, S.M. Pyke, K.K. Sarma, E.R.T. Tiekink, Main Group Met. Chem. 19 (1996) 807.
[18] T.S. Basu Baul, S. Dhar, S.M. Pyke, E.R.T. Tiekink, E. Rivarola, R. Butcher, F.E. Smith, J. Organomet. Chem. 633 (2001) 7.
[19] T.S. Basu Baul, K.S. Singh, X. Song, A. Zapata, G. Eng, A. Lycka, A. Linden, J. Organomet. Chem. 689 (2004) 4702.
[20] R. Hooft, KappaCCD Collect Software, Nonius BV, Delft, The Netherlands, 1999.
[21] Z. Otwinowski, W. Minor, in: C.W. Carter Jr., R.M. Sweet (Eds.), Methods in Enzymology, Macromolecular Crystallography, Part A, vol. 276, Academic Press, New York, 1997, pp. 307–326.
[22] R.H. Blessing, Acta Crystallogr. Sect A 51 (1995) 33.
[23] A. Altomare, G. Cascarano, C. Giacovazzo, A. Guagliardi, M.C. Burla, G. Polidori, M. Camalli, SIR92, J. Appl. Crystallogr. 27 (1994) 435.
[24] G.M. Sheldrick, SHELXS-97, Program for the Solution of Crystal Structures, University of Göttingen, Göttingen, Germany, 1997.
[25] G.M. Sheldrick, SHELXL-97, Program for the Refinement of Crystal Structures, University of Göttingen, Göttingen, Germany, 1997.
[26] A.L. Spek, PLATON, Program for the Analysis of Molecular Geometry, University of Utrecht, The Netherlands, 2007.
[27] S. Dashuang, H. Shengzhi, Chin. J. Struct. Chem. 6 (1987) 193.
[28] F.H. Allen, Acta Crystallogr. Sect. B 58 (2002) 380.
[29] P.F.R. Ewings, P.G. Harrison, T.J. Morris, J. Chem. Soc., Dalton Trans. (1976) 1602.
[30] R.V. Parish, in: G.J. Long (Ed.), Mössbauer Spectroscopy Applied to Inorganic Chemistry, Plenum Press, New York, 1984, pp. 527–575 (Chapter 16).
[31] C. Di Nicola, A. Galindo, J.V. Hanna, F. Marchetti, C. Pettinari, R. Pettinari, E. Rivarola, B.W. Skelton, A.H. White, Inorg. Chem. 44 (2005) 3094.